Physics of the Solid State, Vol. 47, No. 8, 2005, pp. 1497–1503. Translated from Fizika Tverdogo Tela, Vol. 47, No. 8, 2005, pp. 1440–1446.

PROCEEDINGS OF THE XII FEOFILOV WORKSHOP "SPECTROSCOPY OF CRYSTALS ACTIVATED BY RARE-EARTH AND TRANSITION-METAL IONS"

(Yekaterinburg, Russia, September 22–25, 2004)

Stark Structure and Exchange Splittings of Nd^{3+} Ion Levels in Chain Nickelate Nd_2BaNiO_5

M. N. Popova*, E. A. Romanov*, S. A. Klimin*, E. P. Chukalina*, B. V. Mill, and G. Dhalenne*****

**Institute of Spectroscopy, Russian Academy of Sciences, Troitsk, Moscow oblast, 142190 Russia*
e-mail: popova@isan.troitsk.ru
***Moscow State University, Vorob'evy gory, Moscow, 119899 Russia*
****Laboratoire de Physico-Chimie de l'Etat Solide, Université Paris-Sud, Orsay, F-91405 France*

Abstract—Diffusion transmittance spectra of polycrystalline samples of chain nickelate Nd_2BaNiO_5 were measured with high resolution (0.1 cm^{-1}) over wide ranges of wavenumbers (1500–20000 cm^{-1}) and temperatures (4.2–300 K). The energies of 54 Stark sublevels of the Nd^{3+} ion and exchange splittings of some of them were determined in the magnetically ordered state of Nd_2BaNiO_5 ($T_N = 47.5 \pm 1$ K). It was shown that the low-temperature magnetic properties of Nd_2BaNiO_5 are determined by exchange splitting (32 cm^{-1}) of the ground state. © *2005 Pleiades Publishing, Inc.*

1. INTRODUCTION

Due to their structural properties, chain nickelates R_2BaNiO_5 [R is a rare-earth (RE) ion or Y] are interesting model objects for studying one-dimensional magnetism in the system of antiferromagnetic (AFM) chains of atoms with an integer spin ($S = 1$ for Ni^{2+}) and the crossover to three-dimensional magnetic order. As is known, one-dimensional isotropic (Heisenberg) magnets are not ordered even at $T = 0$, because the order is destroyed by fluctuations. In 1983, Haldane showed theoretically that the properties of Heisenberg AFM atomic chains depend strongly on whether the atomic spins are integer or half-integer [1]. In the former case, the ground state is a nonmagnetic singlet and there is a gap in the magnetic excitation spectrum (the Haldane gap). The conclusions reached by Haldane have been confirmed by numerical simulations and experiments with $Ni(C_2H_8N_2)_2NO_2ClO_4$ (NENP) and $CsNiCl_3$ compounds (see, e.g., [2, 3]). Nickelates R_2BaNiO_5 allow smooth variation of the interchain interaction by replacing or partially replacing the rare-earth R^{3+} ion with the nonmagnetic Y^{3+} ion, which offers new opportunities for studying quasi-one-dimensional Haldane magnets.

Nickelates R_2BaNiO_5 (R = Pr–Tm, Y) belong to the orthorhombic crystal system and have space group *Immm* (D_{2h}^{25}) [4, 5]. The most distinctive feature of the structure is the existence of isolated chains (parallel to each other and to the *a* axis) of compressed NiO_6 octahedra connected together by shared vertices (Fig. 1). The chains are bound to each other via Ba^{2+} and R^{3+} ions. The R^{3+} ions occupy equivalent positions with local symmetry C_{2v} (Fig. 1b). The compound with R = Y (Y_2BaNiO_5) is not ordered at least down to 100 mK [6]. The temperature dependence of its magnetic susceptibility is described by a curve with a wide peak typical of a one-dimensional antiferromagnet (the intrachain interaction was estimated from this curve to be $J \approx$ 25 meV [7]). Neutron inelastic scattering spectra reveal an excitation with energy $\Delta \approx 10$ meV, which is attributed to the Haldane gap [7]. The upper estimate of the interchain interaction J' was found in [8] to be $J'/J \leq 5 \times 10^{-4}$. Thus, Y_2BaNiO_5 is an almost ideal model of the AFM chain of spins $S = 1$. The substitution of a RE element for nonmagnetic yttrium causes an increase in the interchain interaction and the onset of magnetic ordering. The magnetic structure of both the nickel and RE subsystem is characterized by a wave vector $\mathbf{k} = (1/2, 0, 1/2)$ for all compounds with $R \neq$ Y [9]. However, the directions of the magnetic moments are different in compounds with different RE elements. For R = Nd, Tb, Dy, and Ho, the magnetic moments are parallel to the *c* axis of the crystal [9], whereas in the Er_2BaNiO_5 compound they are parallel to the *a* axis [9, 10]. The Néel temperatures T_N vary from 12.5 K for Tm_2BaNiO_5 to 65 K for Tb_2BaNiO_5. For Nd_2BaNiO_5, $T_N = 48$ K [9, 11, 12]. For the $(R_xY_{1-x})_2BaNiO_5$ systems ($0 \leq x \leq 1$), $T_N(x)$ varies gradually, which makes it possible to study in detail the crossover from a one-dimensional (1D) quantum antiferromagnet to a three-dimensional (3D) classical antiferromagnet and the behavior of Haldane excitations during the 1D–3D crossover.

Such a study was carried out in [13, 14] for $(Nd_xY_{1-x})_2BaNiO_5$ using neutron inelastic scattering.

1063-7834/05/4708-1497$26.00 © 2005 Pleiades Publishing, Inc.

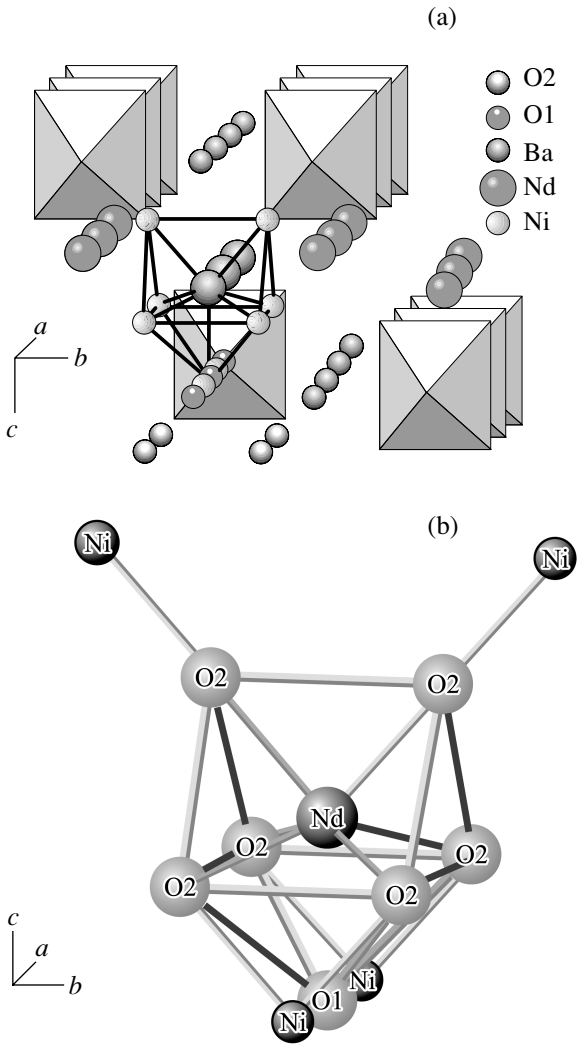

Fig. 1. (a) Structure of Nd_2BaNiO_5 and (b) the nearest neighborhood of the Nd^{3+} ion in Nd_2BaNiO_5. NdO_7 octahedra are bound to each other by shared apical oxygen in chains along the *a* axis. Two octahedra are removed to show the Ni–O–Ni bond in the chains.

Another neutron experiment (for Nd_2BaNiO_5) was performed in [15] with the aim of studying the interaction of 1D magnetic excitations of Ni chains with electronic excitations of the RE subsystem. Interference of these two types of excitation was detected and qualitatively explained. As indicated in [15], the development of a more comprehensive theory of this phenomenon is complicated by the lack of data on the Nd^{3+} electronic states in Nd_2BaNiO_5.

These data are also needed to explain the magnetic properties of Nd_2BaNiO_5. The temperature dependence of the magnetic susceptibility $\chi(T)$ exhibits a very weak feature at the magnetic ordering temperature $T_N = 48$ K [11, 16, 17] and a pronounced peak at a significantly lower temperature, $T_{max} = 26$ K [11, 17], whereas, according to the neutron scattering data, no changes in the magnetic structure are observed. Probably, the peak in the $\chi(T)$ dependence corresponds to depletion of the upper component of the Nd^{3+} Kramers doublet, which is split by exchange interactions in the magnetically ordered state, as is the case in Er_2BaNiO_5 [11, 18]. To test this hypothesis, spectroscopic studies are required.

To our knowledge, the spectroscopic information on the Nd_2BaNiO_5 compound is restricted to the positions of the three lowest Stark sublevels of the ground state (144, 192, 304 cm^{-1}), which were determined using neutron inelastic scattering spectra measured with a resolution of ≈2.5 cm^{-1} [15]. This study is devoted to optical high-resolution (0.1 cm^{-1}) spectroscopy of the Nd_2BaNiO_5 compound and, for comparison, Nd_2BaNiO_5.

2. EXPERIMENTAL

Polycrystalline Nd_2BaNiO_5 and $Nd_{0.1}Y_{1.9}BaNiO_5$ samples were prepared using solid-phase synthesis from powders of Y_2O_3 (99.99%) and/or Nd_2O_3 (99.99%), NiO (99.99%), and $BaCO_3$ (99.99%), which were mixed and annealed at 900°C in air for 24 h and then pelletized under a pressure of 2500 bar. Particular attention was paid to the volatile components in Nd_2O_3 (~15%). Pellets were sintered at temperatures from 1000°C to 1450°C in air for 24–50 h with intermediate grinding. After each treatment, samples were studied using an x-ray diffractometer. After sintering at 1450°C, no impurity phases were detected in the $Nd_{0.1}Y_{1.9}BaNiO_5$ sample and the diffraction pattern corresponded to space group *Immm*. The diffraction pattern of Nd_2BaNiO_5 after treatment at 1350°C also showed the group *Immm*; however, traces of other phases were observed.

High-resolution (to 0.1 cm^{-1}) diffusion transmittance spectra of Nd_2BaNiO_5 samples were measured over wide spectral (1600–20000 cm^{-1}) and temperature (4.2–300 K) ranges using a high-resolution AIIAI DA3.002 Fourier spectrometer. Powder samples were mixed with ethanol and applied onto a BaF_2 substrate. Then, the sample was placed into a cryostat with helium vapor. A silicon detector was used for the spectral range 9000–20000 cm^{-1}. Two InSb detectors were used for the range 5000–10000 cm^{-1}. One of them was conventional; the other, special, detector was positioned in the cryostat immediately behind the sample. The range 1600–5000 cm^{-1} was studied using a mercury–cadmium–tellurium detector.

3. OPTICAL SPECTRA OF $Nd_{0.1}Y_{1.9}BaNiO_5$ AND Nd_2BaNiO_5 IN THE PARAMAGNETIC STATE AND THE STARK STRUCTURE OF THE Nd^{3+} ION LEVELS

Figure 2 shows the general transmittance spectrum of polycrystalline Nd_2BaNiO_5 samples in the paramagnetic state. Narrow lines correspond to the *f–f* transitions in the Nd^{3+} ion from the $^4I_{9/2}$ ground state to excited levels. For comparison, the positions of the Nd^{3+} levels in $LaCl_3$ [19] are shown. The positions of the lower levels $^4I_{11/2}$, $^4I_{13/2}$, and $^4I_{15/2}$ are identical for Nd_2BaNiO_5 and $LaCl_3$, while the higher levels of Nd_2BaNiO_5 are shifted to lower energies in comparison with those of $LaCl_3$. This nephelometric shift [20, 21] in Nd_2BaNiO_5 is caused by the strong overlap of the wave functions of the Nd^{3+} excited states with the ligand wave functions.

In the crystal field with C_{2v} local symmetry, each level of the free Nd^{3+} ion with a total angular momentum J is split into $J + 1/2$ Kramers doublets (see the diagram in Fig. 3). All spectra can be interpreted in terms of a single neodymium center. To facilitate analysis of the Stark splittings, we used the diluted $Nd_{0.1}Y_{1.9}BaNiO_5$ compound, which is not ordered at least down to 10 K and whose spectrum is not complicated by exchange splittings. The transmittance spectra of both compounds are compared in Fig. 4. The Stark sublevel energies of the Nd^{3+} ion multiplets as determined from the spectra are listed in the table. The Stark sublevels of the $^4I_{9/2}$ ground state were determined from transmittance spectra at elevated temperatures (Fig. 5). The intensities of the lines that become stronger as the temperature increases correlate with the population of the excited Stark sublevels of the ground state (Fig. 6). The energies of the lowest levels thus determined (140, 190, 302 cm^{-1}) agree well with the neutron scattering data (144, 192, 304 cm^{-1}) [15].

The experimentally determined positions of 54 Stark levels of the Nd^{3+} ion in Nd_2BaNiO_5 can be used for performing an analysis in terms of crystal field theory.

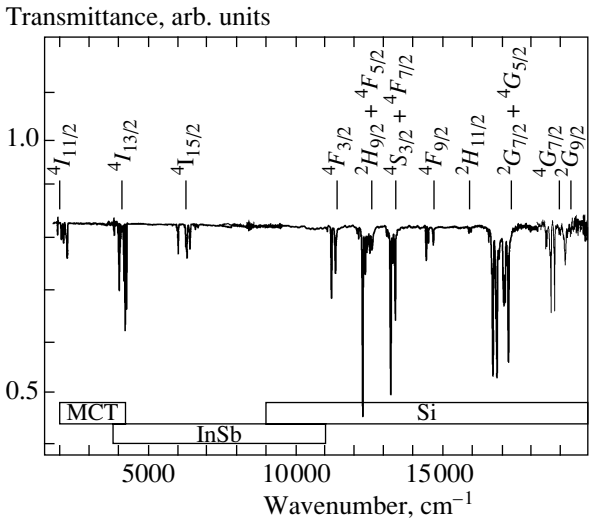

Fig. 2. Transmittance spectrum of Nd_2BaNiO_5 at ~100 K. The operational spectral ranges of the radiation detectors employed are indicated at the bottom (MCT stands for mercury–cadmium–tellurium). The positions of the Nd^{3+} ion multiplets in the $LaCl_3 : Nd^{3+}$ compound are shown at the top [19].

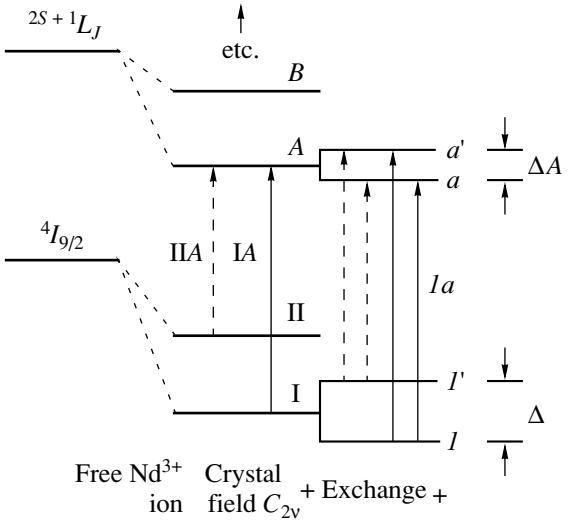

Fig. 3. Schematic diagram of the Nd^{3+} level splitting in the crystal field and of the Kramers doublet splitting in the magnetically ordered state. The optical transitions frozen out at low temperatures are indicated by dashed lines.

4. EXCHANGE SPLITTINGS IN Nd_2BaNiO_5 SPECTRA: MOLECULAR-FIELD MODEL

In the magnetically ordered state, magnetic interactions remove the Kramers degeneracy of Nd^{3+} ions, which results in a splitting of spectral lines (Fig. 3). Figure 7 shows the variation of one of the lines as the temperature is lowered. The splitting arising at ~50 K increases and the lines narrow. At $T \le 35$ K, all four components of the split line are clearly visible, with the low-frequency components being "frozen out." By analyzing the spectra, we can determine the exchange splittings (due to magnetic ordering) of the Kramers doublets corresponding to the initial and final levels of an optical transition. The splittings as determined from the spectra at $T = 5$ K are listed in the table.

Figure 8 shows the temperature dependences of the ground-state splitting $\Delta(T)$, of the energy of the 4-meV mode detected in the neutron scattering spectrum [14], and of the magnetic moment of the nickel subsystem

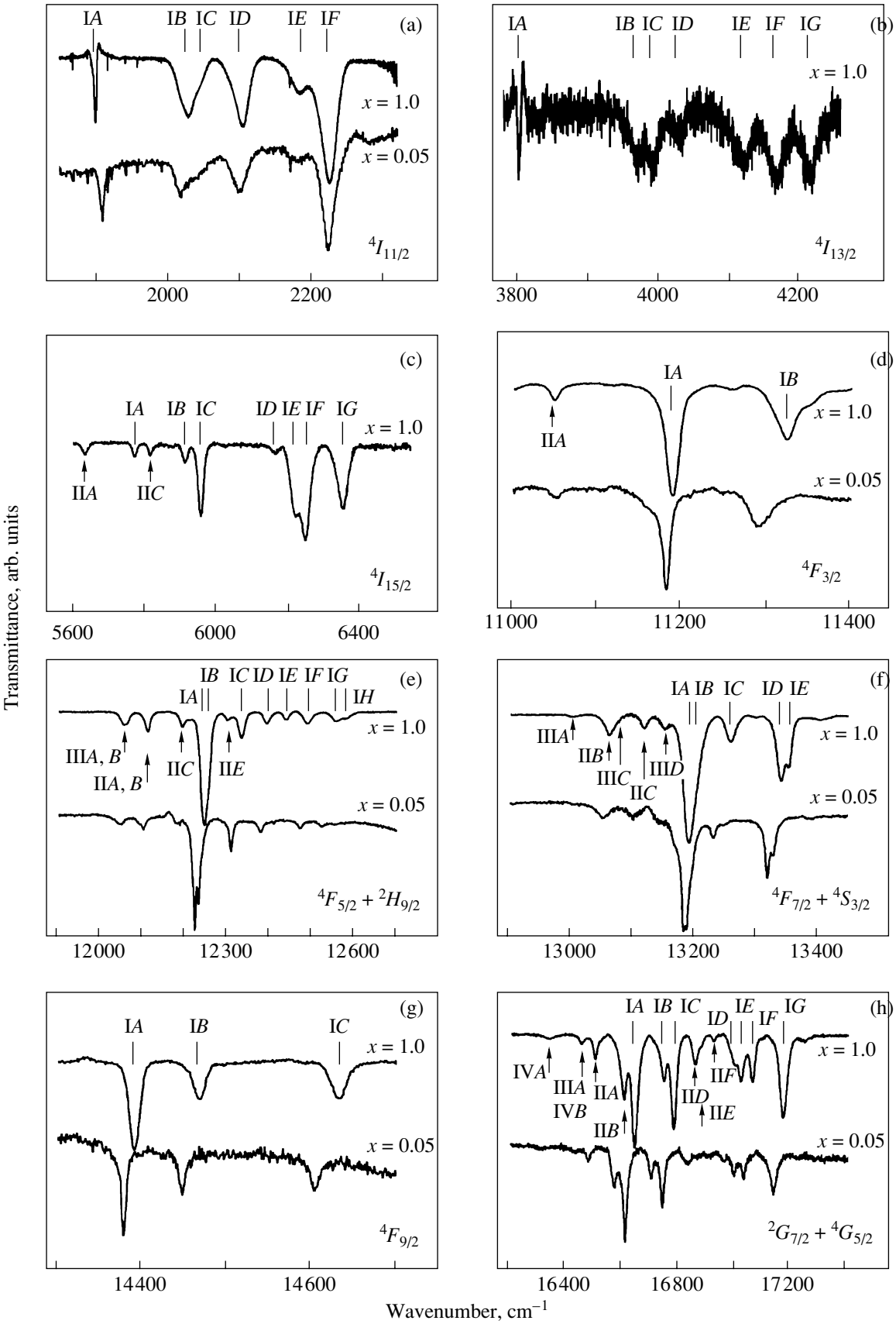

Fig. 4. Transmittance spectra of $(Nd_xY_{1-x})_2BaNiO_5$ at 100 K in the range of transitions from the $^4I_{9/2}$ ground state of the Nd^{3+} ion to excited states (indicated in the right bottom of each panel). Spectral lines are denoted according to the notation in Fig. 3.

Stark level energies of the Nd^{3+} ion in chain nickelates $(Nd_xY_{1-x})_2BaNiO_5$ determined from the transmittance spectra at $T = 90$ K; the exchange splittings (cm^{-1}) for Nd_2BaNiO_5 at $T = 5$ K are given in parentheses

Multiplet	E, cm^{-1}		Multiplet	E, cm^{-1}	
	$x = 1$	$x = 0.05$		$x = 1$	$x = 0.05$
$^4I_{9/2}$	0 (32)	0	$^4F_{5/2}$	12241 (<2)	12222
	140	130		12251 (<2)	12231
	190	180		12330 (3.7)	12306
	302	290	$^2H2_{9/2}$	12390	12377
	~440	440		12438	12410
$^4I_{11/2}$	1901	1909		12490	12470
	2029	2018		12552	12521
	2046	2040		12580	12551
	2104	2100	$^4F_{7/2}$	13190 (5.3)	13183
	2183	2178		13200 (5.3)	13187
	2224	2222		13258 (4)	13229
$^4I_{13/2}$	3807		$^4S_{3/2}$	13340 (14.5)	13318
	3970	3956		13352 (22)	13327
	3992 (11)	3978	$^4F_{9/2}$	14390 (2)	14379
	4029	4022		14468 (7)	14447
	4119	4117		14631 (14)	14603
	4169	4160	$^4G_{5/2}$	16640 (6)	16608
	4217	4212		16743 (10)	16699
$^4I_{15/2}$	5772			16779 (7)	16738
	5912 (16)		$^2G_{7/2}$	16996	16992
	5956 (<4)			17015	17026
	6163			17057	
	6220			17168	17132
	6248		$^4G_{7/2}$	18585	18600
	6353			18625	18704
$^4F_{3/2}$	11188 (11.4)	11182		18748	
	11323	11290	$^2G_{9/2}$	19114	

$m_{Ni}(T)$ determined from the neutron scattering data [14]. The 4-meV mode in Nd_2BaNiO_5 observed in neutron scattering experiments was initially assigned to the Stark level of the Nd^{3+} ion [22]. However, it is clearly seen from Fig. 8 that, in actual fact, this mode corresponds to the transition between the components of the Nd^{3+} ground-state Kramers doublet split by the magnetic interaction in the magnetically ordered state, i.e., to the neodymium magnetic moment being flipped, as expected in [12].

For $T < 0.9T_N$, the splitting of the RE-ion ground state in Nd_2BaNiO_5 is proportional to the magnetic moment of the nickel subsystem (Fig. 8), as in the case of Er_2BaNiO_5 [11, 18]. Therefore, the molecular-field model is applicable to this system, according to which the RE ions are subject to the effective magnetic field B_{eff} induced by the ordered nickel subsystem [11, 17, 18]. Within this approximation, we can write

$$\Delta(T) = 2m_{Nd}^{(0)}B_{eff}(T), \quad (1)$$

$$B_{eff}(T) = \lambda m_{Ni}(T). \quad (2)$$

where $m_{Nd}^{(0)}$ is the magnetic moment of the Nd^{3+} ion in the ground state and λ is the molecular-field constant. Using the experimental values $m_{Nd}^{(0)} = 2.65\mu_B$ and $m_{Ni}^{(0)} = 1.6\mu_B$ (derived from the neutron scattering data [9]) and fitting the experimental $\Delta(T)$ dependence with Eqs. (1) and (2), we obtain $\lambda = 7.61\mu_B$. This value agrees well with the value $\lambda = 7.51\mu_B$ obtained in [17] by analyzing the Nd_2BaNiO_5 magnetic susceptibility.

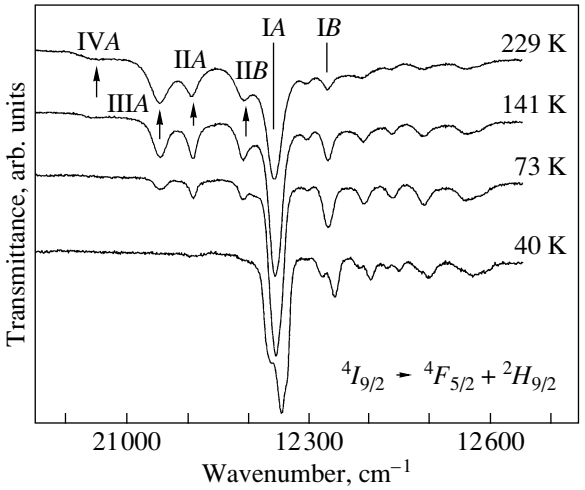

Fig. 5. Transmittance spectrum of Nd_2BaNiO_5 at various temperatures. The lines corresponding to transitions from the excited sublevels of the $^4I_{9/2}$ multiplet disappear as the temperature decreases. At 40 K, one can see exchange splittings of the I*A* and I*B* lines.

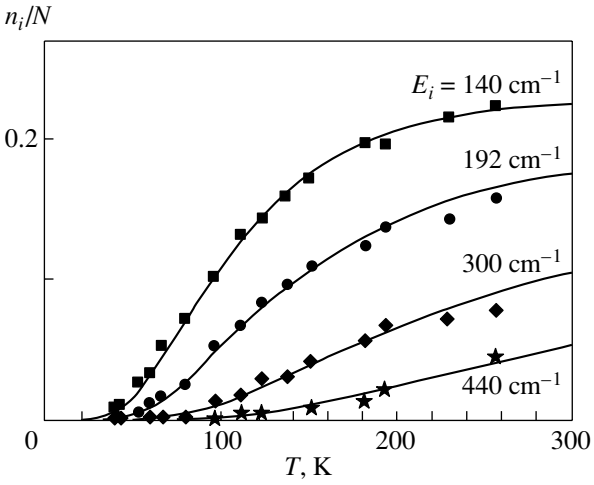

Fig. 6. Populations of excited levels with energy $E_i$as calculated using the formula $n_i/N = \exp(-E_i/kT)/\sum_{j=1}^{5}\exp(-E_j/kT)$ (solid curves) and experimentally measured intensities of spectral lines (dots).

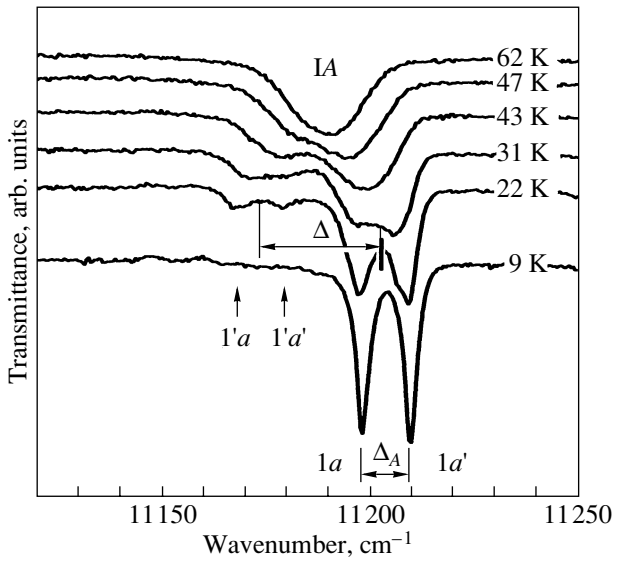

Fig. 7. Line I*A* (Fig. 4d) at various temperatures. The notation corresponds to that in Fig. 3.

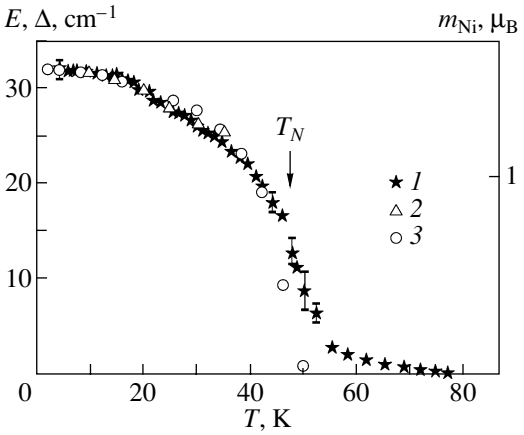

Fig. 8. Temperature dependences of (*1*) the splitting Δ of the Nd^{3+} ion ground state, (*2*) the energy *E* of the 4-meV mode observed in the neutron scattering spectrum, and (*3*) the magnetic moment m_{Ni}. The Δ(*T*) dependence was obtained from the spectroscopic measurements in this study, and *E*(*T*) and $m_{Ni}(T)$ were plotted using the experimental data on neutron scattering [14].

At $T > T_N$, the spectral line splitting does not disappear completely. The remaining splitting is associated with the short-range order. Previously, we assumed that the magnetic ordering temperature could be determined from the position of the inflection point in the Δ(*T*) dependence [23, 24]. A comparison of the optical and neutron scattering data for Nd_2BaNiO_5 (Fig. 8) confirms this assumption. Based on the spectroscopic data, we obtained $T_N = 47.5 \pm 1$ K, which agrees with T_N = 48 K determined from neutron diffraction studies [9, 16].

5. MAGNETIC MOMENT OF THE NEODYMIUM SUBSYSTEM IN MAGNETICALLY ORDERED Nd_2BaNiO_5

The excited Stark sublevels of the ground-state multiplet (140, 190 cm^{-1}, etc.; see table) are almost empty at $T < T_N$. Therefore, only the ground-state Kramers doublet contributes to the magnetic moment m_{Nd} of the neodymium subsystem and we can write

$$m_{Nd}(T) = m_{Nd}^{(0)}\frac{n_1 - n_2}{n_1 + n_2} = m_{Nd}^{(0)}\tanh\frac{\Delta(T)}{2kT}. \qquad (3)$$

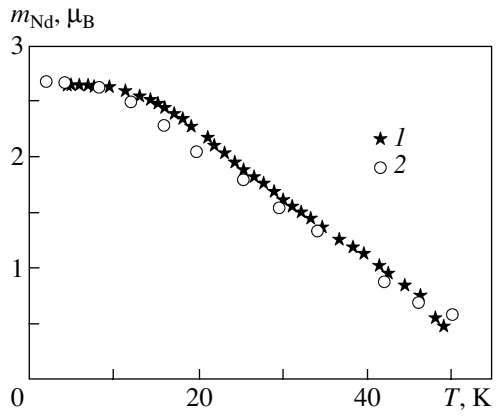

Fig. 9. Temperature dependences of the Nd^{3+} magnetic moment in the magnetically ordered state of Nd_2BaNiO_5 as obtained (*1*) from the spectroscopic data using Eq. (3) and (*2*) from neutron scattering data.

where $m_{Nd}(T)$is the magnetic moment per Nd^{3+} ion and n_1 and $n_2 = n_1\exp(\Delta/kT)$ are the populations of the lower and upper sublevels of the ground-state Kramers doublet.

Figure 9 shows the $m_{Nd}(T)$ dependences calculated from Eq. (3) using the spectroscopic data on the ground-state splitting $\Delta(T)$ and found from the neutron scattering data [14]. The good agreement confirms the applicability of the spectroscopic technique for studying the magnetic properties of chain nickelates.

The data obtained in this study also directly substantiate the approach (proposed for the first time in [11]) applied in [17] to calculate the magnetic susceptibility $\chi(T)$ of Nd_2BaNiO_5. Moreover, these data show that the peak in the $\chi(T)$ dependence at a temperature $T_{max} \sim$ 26 K (or at 30 K, according to [11]), which is significantly lower than the magnetic ordering temperature $T_N = 47.5$ K, is caused by depletion of the upper component of the Nd^{3+} ion ground-state Kramers doublet split by Nd–Ni interactions in magnetically ordered Nd_2BaNiO_5. Using this approach, the temperature of this peak can be estimated from the formula $kT_{max} = 0.65\Delta(0)$ without calculating the entire $\chi(T)$ dependence [23]. By substituting $\Delta(0) = 32$ cm^{-1} determined from the spectra, we obtain an estimate $T_{max} = 30$ K that is close to the observed value.

ACKNOWLEDGMENTS

This study was supported by the Russian Foundation for Basic Research (project no. 04-02-17346) and the Russian Academy of Sciences (fundamental research programs).

REFERENCES

1. F. D. M. Haldane, Phys. Rev. Lett. **50** (15), 1153 (1983).
2. W. J. L. Buyers, R. M. Morra, R. L. Armstrong, M. J. Hogan, P. Gerlach, and K. Hirakawa, Phys. Rev. Lett. **56** (4), 371 (1986).
3. Z. Tun, W. J. L. Buyers, A. Harrison, and J. A. Rayne, Phys. Rev. B **43** (16), 13 331 (1991).
4. S. Schiffler and H. Müller-Buschbaum, Z. Anorg. Allg. Chem. **532**, 10 (1986).
5. E. García-Matres, J. L. Martínez, and J. Rodríguez-Carvajal, J. Solid State Chem. **103**, 322 (1993).
6. K. Kojima, A. Keren, L. P. Le, G. M. Luke, B. Nachumi, W. D. Wu, Y. J. Uemura, K. Kiyono, S. Miyasaka, H. Takagi, and S. Uchida, Phys. Rev. Lett. **74** (17), 3471 (1995).
7. J. Darriet and L. P. Regnault, Solid State Commun. **86** (7), 409 (1993).
8. Guangyong Xu, J. F. Ditusa, T. Ito, K. Oka, H. Takagi, C. Broholm, and G. Aeppli, Phys. Rev. B **54** (10), 6827 (1996).
9. E. García-Matres, J. L. Martínez, and J. Rodríguez-Carvajal, Eur. Phys. J. B **24**, 59 (2001).
10. K. A. Alonso, J. Amador, J. L. Martinez, I. Rasines, J. Rodríguez-Carvajal, and R. Saez-Puche, Solid State Commun. **76** (4), 467 (1990).
11. G. G. Chepurko, Z. A. Kazei, D. A. Kudrjavtsev, R. Z. Levitin, B. V. Mill, M. N. Popova, and V. V. Snegirev, Phys. Lett. A **157** (1), 81 (1991).
12. A. Zheludev, J. M. Tranquada, T. Vogt, and D. J. Buttrey, Phys. Rev. B **54** (9), 6437 (1996).
13. T. Yokoo, A. Zheludev, M. Nakamura, and J. Akimitsu, Phys. Rev. B **55** (17), 11 516 (1997).
14. T. Yokoo, S. A. Raymond, A. Zheludev, S. Maslov, E. Ressouche, I. Zaliznyak, R. Erwin, M. Nakamura, and J. Akimitsu, Phys. Rev. B **58** (21), 14 424 (1998).
15. A. Zheludev, S. Maslov, T. Yokoo, J. Akimitsu, S. Raymond, S. E. Nagler, and K. Hirota, Phys. Rev. B **61** (17), 11 601 (2000).
16. A. Zheludev, J. P. Hill, and D. J. Buttrey, Phys. Rev. B **54** (10), 7216 (1996).
17. E. García-Matres, J. L. García-Munos, J. L. Martínez, and J. Rodríguez-Carvajal, J. Magn. Magn. Mater. **149**, 363 (1995).
18. M. N. Popova, S. A. Klimin, E. P. Chukalina, B. Z. Malkin, R. Z. Levitin, B. V. Mill, and E. Antic-Fedancev, Phys. Rev. B **68** (15), 155103 (2003).
19. G. H. Dieke, *Spectra and Energy Levels of Rare Earth Ions in Crystals* (Interscience, New York, 1968), p. 142.
20. P. Caro, O. Beaury, and E. Antic, J. Phys. (France) **37**, 671 (1976).
21. E. Antic-Fidancev, M. Lemaitre-Blaise, and P. Caro, New J. Chem. **11** (6), 467 (1987).
22. A. Zheludev, J. M. Tranquada, T. Vogt, and D. J. Buttrey, Phys. Rev. B **54** (10), 7210 (1996).
23. M. N. Popova, Proc. SPIE **2706**, 182 (1996).
24. M. N. Popova, J. Alloys Compd. **275-277**, 142 (1998).

Translated by A. Kazantsev

SPELL: OK